

# Surface strain distribution of orthodontic miniscrews under load

Prapaporn Shantavasinkul,<sup>a</sup> Ozan Akkus,<sup>b</sup> J. Martin Palomo,<sup>c</sup> and Sebastian Baumgaertel<sup>d</sup>  
Cleveland, Ohio

**Introduction:** Our objective was to investigate surface strain around orthodontic miniscrews under different orthodontic loading conditions in simulated supporting bone. **Methods:** Thirty miniscrews with lengths of 6, 8, and 10 mm were embedded into customized composite analog bone models. All miniscrews were inserted into the simulated test bone 6 mm deep and loaded with the same force of 200 cN, creating different tipping moments at the peri-implant bone surface. A digital image correlation technique was used to measure the resulting surface strain around the orthodontic miniscrews. **Results:** Changing the tipping moments is directly related to the strain generated at the bone surface close to the miniscrews, with greater moments creating greater maximum principal strains. **Conclusions:** Within the limitations of this model, it can be stated that greater tipping moments of miniscrews create greater maximum principal strain values, which have the potential to increase bone turnover around the implant. Hence, miniscrews farther from the bone surface should be loaded with less force, whereas miniscrews loaded closer to the bone surface may sustain higher forces. (Am J Orthod Dentofacial Orthop 2016;150:444-50)

Unless there is peri-implantitis, a negatively imbalanced biomechanical environment in the adjacent bone tissue is the main assumption for miniscrew failure.<sup>1</sup> Therefore, understanding how functional loads are transferred to the bone-miniscrew interface will help to determine the best prognosis of stability for orthodontic anchorage. Although miniscrews can be loaded immediately without impairing stability and reducing success rates, Büchter et al<sup>2</sup> showed that increased miniscrew failures under immediate loading appear to be directly related to the tipping moment at the bone rim.

More recently, an interest in bone biomechanics has developed by authors who found that bone failure by fracture was driven by deformation and strain-based

conditions, which can predict fracture sites.<sup>3-5</sup> The influence of strain distribution on the success of dental implants is undisputed and has been known for decades; however, less is known about specific thresholds of strain parameters related to the success of miniscrews. A recent subject-specific finite element analysis (FEA) study of miniscrews demonstrated that the maximum principal strain is the most reliable parameter for predicting miniscrew failure.<sup>6</sup> Because FEA modeling depends on many assumptions and represents a simplification of actual conditions, it has the shortcoming of being a simulation of clinical parameters with inherent inaccuracies. To date, no authors have actually measured strain distributions around orthodontic miniscrews at different loads.

Digital image correlation is an optical full field for noncontact, 3-dimensional (3D) deformation measurement that has been developed to measure displacement and surface strain distribution in materials testing.<sup>7</sup> It is particularly suitable for biologic applications because it can be used accurately to determine strain in inhomogeneous, anisotropic, nonlinear materials such as bone. Several studies have used the digital image correlation method to analyze the biomechanics of an implant-supported prosthesis.<sup>8,9</sup> Digital image correlation can simultaneously measure 3D displacements in a high dynamic range (nanometers to millimeters) and has low intrasample variations of the surface strain while reconstructing the surface accurately.<sup>10</sup>

From Case Western Reserve University, Cleveland, Ohio.

<sup>a</sup>Resident, Department of Orthodontics, School of Dental Medicine.

<sup>b</sup>Professor, Orthopaedic Bioengineering Laboratories, Department of Mechanical and Aerospace Engineering.

<sup>c</sup>Professor and residency director, Department of Orthodontics, School of Dental Medicine.

<sup>d</sup>Clinical associate professor, Department of Orthodontics, School of Dental Medicine.

All authors have completed and submitted the ICMJE Form for Disclosure of Potential Conflicts of Interest, and none were reported.

Address correspondence to: Sebastian Baumgaertel, Department of Orthodontics, School of Dental Medicine, Case Western Reserve University, 10900 Euclid Ave, Cleveland, OH 44106; e-mail, [dr.b@us-ortho.com](mailto:dr.b@us-ortho.com).

Submitted, August 2015; revised and accepted, February 2016.

0889-5406/\$36.00

© 2016 by the American Association of Orthodontists. All rights reserved.

<http://dx.doi.org/10.1016/j.ajodo.2016.02.019>

Therefore, the purpose of this in-vitro study was to analyze strains generated by miniscrews under continuously applied orthodontic loads in simulated supporting bone by creating different tipping moments, mimicking various clinical situations.

## MATERIAL AND METHODS

Thirty self-drilling miniscrews (Tomas SD; Dentaurum, Ispringen, Germany) with lengths of 6, 8, and 10 mm and a diameter of 1.6 mm were used in this study. Half of the miniscrews were assigned to strain testing on the compression side, and the other half were assigned to strain testing on the noncompression side (Table 1).

For the simulated bone blocks, customized composite analog bone models (Sawbones; Pacific Research Laboratories, Vashon Island, Wash) were used to simulate the cortical and cancellous bone. The models were milled to  $11.5 \times 40 \times 20$  mm (height, length, and depth, respectively). Young's modulus values of cortical plate and cancellous bone were 16.7 and 68.4 MPa, respectively.

Digital image correlation analysis comprises 4 consecutive steps: (1) specimen preparation, (2) calibration of the imaging system for a defined field of view, (3) collection of specimen deformation before and after loading, and (4) postprocessing of images to determine displacement or strain.<sup>11</sup>

A specimen is prepared before testing by coating the surface of the composite analog bone model using a high-quality airbrush (Evolution Solo airbrush with a Euro-Tech 10A compressor; Harder & Steenbeck, Oststeinbek, Germany) with airbrush paint (8549 titanium white, high-flow acrylic; Golden Artist Colors, New Berlin, NY) as the background color to improve the contrast between the replicate bone model surface and the speckle pattern. The speckle pattern was applied using airbrush paint (8524 carbon black, high-flow acrylic; Golden Artist Colors). A similar method for speckling samples on a microscale was outlined in a previous study.<sup>12</sup>

A charged-coupled device camera (Correlated Solutions, Columbia, SC) calibration was performed to orient the cameras in 3D space. The calibration process is essential for acquiring accurate 3D measurements.<sup>11</sup> The calibration procedure determines the 3D position of each camera relative to the world coordinate system.

Calibration for the camera setup was carried out with a calibration grid plate (3 mm dot spacing; Correlated Solutions). The calibration plate was displaced in increments in all 3 planes, and images of the calibration target were acquired to calibrate the system.

All composite analog bone models were rigidly stabilized, and 3 images were taken on each experimental

**Table 1.** Experimental design

	Load type	
	Compression	Tension
Miniscrews (n = 30)	15	15
200 cN, 3-mm lever arm (600 cN•mm)	5	5
200 cN, 5-mm lever arm (1000 cN•mm)	5	5
200 cN, 7-mm lever arm (1400 cN•mm)	5	5

procedure (Fig 1). Thirty miniscrews (6, 8, and 10 mm in length) were inserted to a 6-mm depth, regardless of their length, into replicated bone models according to the manufacturer's recommendation (Fig 2). The point of force application was 3 mm from the base of the collar; thus, the distances between the point of force application and bone surface were 3, 5, and 7 mm for the 6-, 8-, and 10-mm miniscrews, respectively. After insertion, each miniscrew was loaded with either a 200-cN push force (Dontrix gauge; Lancer Orthodontics, Vista, Calif) or a 200-cN pull force (200-g load cell). The first image was captured immediately after miniscrew placement, and the second image was taken at least 2 minutes later with the miniscrew under load as described above.

The images were processed using special software (Vic-3D version 7; Correlated Solutions), and the field of view for the area of interest was  $10 \times 10$  mm. Unique correlation areas were defined across the entire imaging area. For each area, the corresponding locations in all other images from the second camera and all loading situations were automatically determined and tracked with subpixel accuracy. The system then used photogrammetric principles to calculate the 3D coordinates of the entire surface in all loading stages to determine displacement or strain.<sup>13</sup>

Five measurement points were selected with increasing distances from the miniscrews along the x-line (0.5, 1.0, 1.5, 2.0, and 2.5 mm) (Fig 3).

## Statistical analysis

All statistical calculations were performed with SPSS software (version 22; IBM, Armonk, NY). The Shapiro-Wilk test was used to determine frequency distribution, and intraclass correlation was used to determine intrarater reliability. Because the distribution was predominantly nonnormal, the Kruskal-Wallis test with the Mann-Whitney *U* test for post hoc analysis was used to test for differences in bone surface strain distribution. The level of significance was set at  $P \leq 0.05$ . Additional post hoc analysis was used to calculate whether the power of the statistical test was effectively performed.

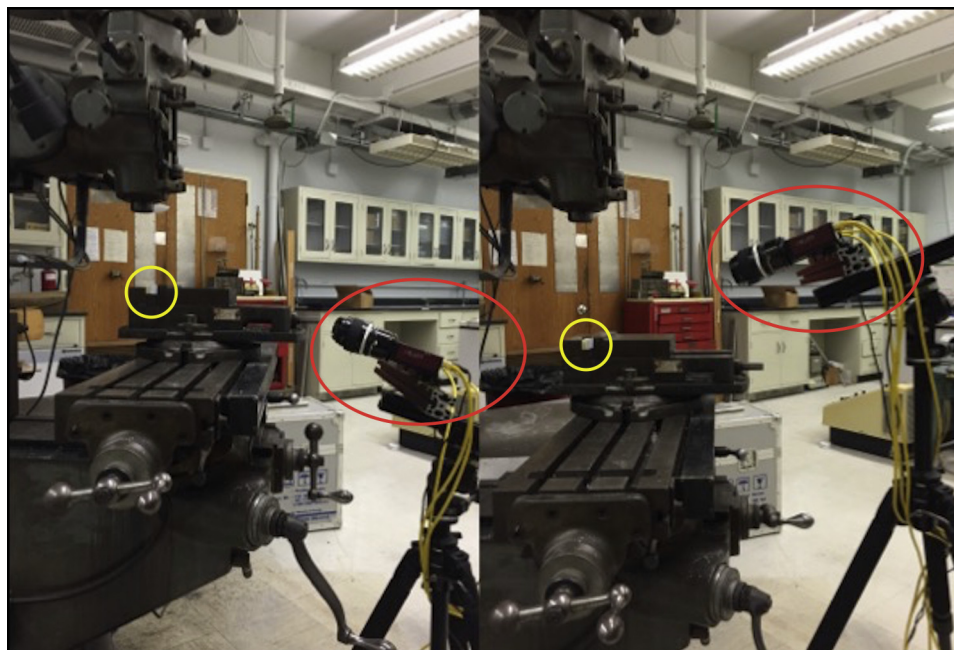


**Fig 1.** Experimental setup with camera orientation for “push” load (*left*) and “pull” load (*right*): positions of the cameras (*red circles*) and artificial bone blocks containing the miniscrews (*yellow circles*).

## RESULTS

Intrarater reliability was high ( $r = 0.92$ ), and the measurements proved to be reproducible. Post hoc analysis in groups with a statistically significant difference ranged from 88% to 100% at 0.5 mm from the orthodontic miniscrews.

Three parameters (maximum principal, minimum principal, and shear strains) were calculated, with mean values and standard deviations shown in Table II.

The direct strain in the vertical direction ( $Y_{axis}$ ) was measured for the 3 groups with pull (Fig 3) and push (Fig 4) forces. Statistical analysis showed that all values of maximum principal strain and minimal principal strain on the compression side at all measuring points were significantly different between the groups ( $P \leq 0.05$ ), and significantly higher levels of maximum principal strain can be seen for the 8-mm and 10-mm groups on the compression side. No significant difference in minimum principal strain was found between the groups on the bone surface of the noncompression side.

Shear strains were calculated and showed statistically significant differences at the region below the mini-implants at all measurement points except for the strains at the 6-mm and 8-mm screws. When we analyzed the area above the miniscrews, there was no statistically significant difference at any measurement point.

When we compared bone surface strains at the different measurement points, the greatest measurements

were recorded closest to the miniscrews, and the smallest values were registered farthest from the miniscrews for all 3 strain parameters.

## DISCUSSION

We used the digital image correlation method to analyze the strain distributions; this provided actual surface strain values rather than computed values from a simulation model, which relies on the assignment of boundary conditions and comes with other system-inherent inaccuracies. Additionally, the digital image correlation method provided low intrasample variations of surface strains,<sup>10</sup> and the repeatability of measuring was great with a variation coefficient of 0.5%.<sup>14</sup>

Our study design aimed to create groups that differed in only 1 variable, to find the actual relationship between strain and tipping moments; hence, we kept the insertion depth and force constant and changed the moment of force using different lengths of miniscrews inserted to the same depth but protruding by different amounts from the surface. This is a clinically relevant question because miniscrews can be loaded with different forces and, at the same time, at different distances to the bone surface because of either different attachment points or collar lengths on the miniscrews or different insertion depths.

For this study, we chose a force level of 200 cN, which we considered a medium load level within the physiologic

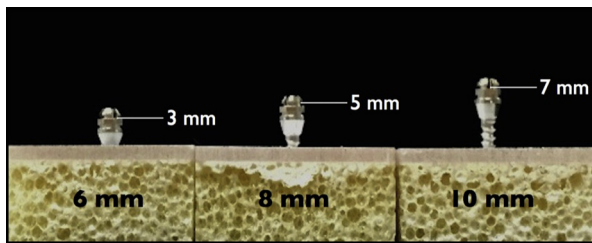


**Fig 2.** Miniscrews inserted into artificial bone blocks (screw lengths, *black font*), including points of force application and distances to the bone surface (*white font*).

load range of 100 to 300 cN, and hence a realistic simulation of a clinical scenario.<sup>15</sup>

It became evident that changing the moment of force directly impacts the strain generated at the bone surface close to a miniscrew. The authors of several studies found similar results, including FEA studies.<sup>1,16</sup> They reported strain concentrations in the marginal peri-implant bone after lateral or oblique load application and showed a significant impact on the biologic activity of the adjacent bone tissue, potentially leading to resorptive remodeling. Our values of maximum principal strain in the 1000 and 1400 cN·mm groups were statistically significantly higher than the group with 600 cN·mm tipping forces. Because increased bone strain increases bone turnover, this suggests that excessive tipping moments may put miniscrews at greater risk for failure; this is similar to the studies of Roberts et al,<sup>17-19</sup> who found that implants remained stable when the applied load ranged from 100 to 300 cN, but they did not account for the distance at which these loads were applied. Furthermore, Buchter et al<sup>2</sup> found that all miniscrews installed in mandibular bone were successfully loaded and remained stable through the entire study, when tipping forces were not higher than 900 cN·mm. Several long-term clinical studies demonstrated that implant failures have been attributed to overloading or excessive loading when no peri-implantitis phenomena were present; this supports our findings. The result of excessive strains and stresses at the bone-implant interface were considered to be the critical factor for implant failure.<sup>1</sup>

In our findings, between maximum principal strain, minimum principal strain, and shear strain, only maximum principal strain had a significant difference between the groups at areas above and below a miniscrew; this may suggest that maximum principal strain can be used for predicting failure of miniscrews.<sup>20</sup> This corroborates other recent studies that proposed to use maximum principal strain as a predictor of miniscrew failure in finite element models. The authors concluded that when the

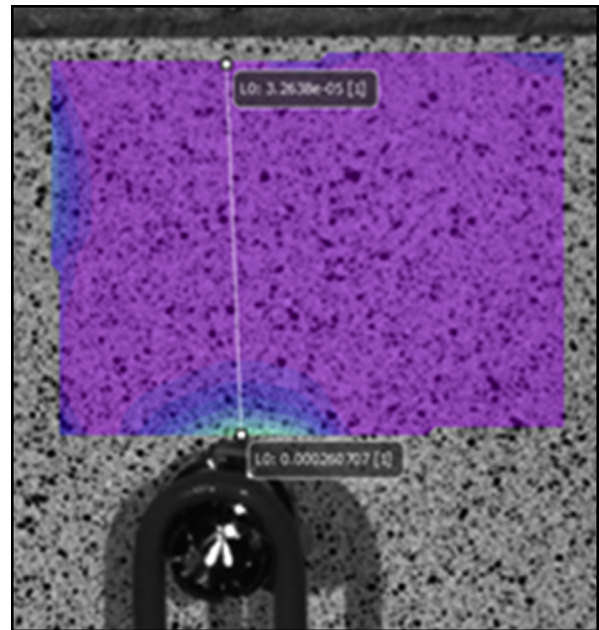


**Fig 3.** “Pull” force application: area of interest above the miniscrew (including the measurement of the x-line).

maximum principal strain is greater than 5785 microstrains, the miniscrew’s probability of failure is greater than 95%, and peak values of maximum principal strain in bone had the highest correlation in miniscrew stability among all strain parameters.<sup>6</sup> This also agrees with a study by Isidor,<sup>20</sup> who showed a long-term basis of failure of osseointegration by occlusal overload. Furthermore, studies have shown that high strain values above 6700 microstrains resulted in 50% peri-implant bone resorption along dental implants with a negative balance during bone remodeling.<sup>20,21</sup> It is believed that a low mechanical load, not exceeding a tolerable strain level, would not be accompanied by bone loss or impaired mineralization.<sup>22,23</sup>

We found that peak strains occur closest to the miniscrews and dissipate with increasing distance. This may come as a surprise, but it can offer another explanation about why the palate is a superior site for miniscrew insertion, with greater success rates,<sup>24</sup> because insertions have a greater distance to anatomic structures than anywhere else in the jaws. This allows for distribution of the strains over a greater area without interaction with other structures.

Von Mises stress<sup>25</sup> is widely used to predict failures of materials regarding whether they will withstand a given load condition and is advocated in many studies to evaluate miniscrews using FEA.<sup>26,27</sup> Recent studies have shown that von Mises stress does not reliably predict the yielding behavior of bone and that the

**Table II.** Means and standard deviations of maximum principal strain values ( $e_1$ ), minimum principal strain values ( $e_2$ ), and shear strain ( $e_{xy}$ ) with push and pull forces 5 mm from the miniscrews

Type of force	Strain parameter	Strain values (microstrains)						P value
		600 cN·mm		1000 cN·mm		1400 cN·mm		
		Mean	SD	Mean	SD	Mean	SD	
Push	$e_1$	-320	48.82	-440	52.8	-647	123.6	0.000*
	$e_2$	-1358	86.0	-2517	547	-2853	123	0.013*
	$e_{xy}$	128	57.61	160	135.09	260	169.22	0.005*
Pull	$e_1$	228	44.04	547	70.73	953	123.59	0.000*
	$e_2$	-18	24.86	10	39.58	17	11.94	0.543
	$e_{xy}$	66	54.20	68	35.10	142	123.30	0.216

\* $P \leq 0.05$ .

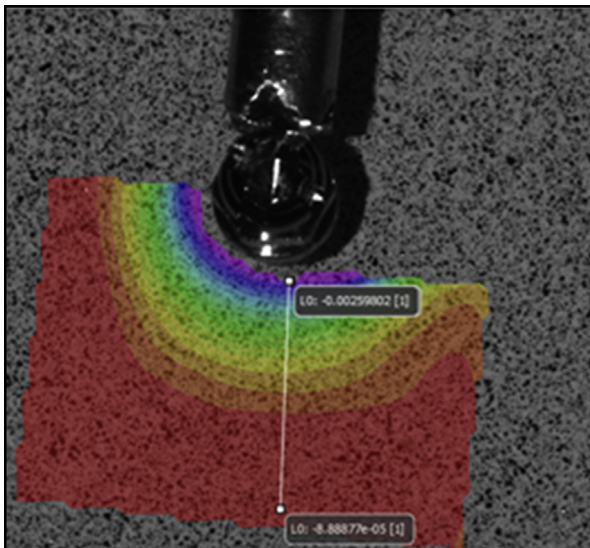


**Fig 4.** “Push” force application: area of interest below the miniscrew.

principal strain criterion correctly identifies the risk of failure.<sup>6,28</sup>

Because almost all of the principal strain values above the miniscrew were tensile strains, it may now be understandable why miniscrews tend to displace in the direction of force after being loaded without an increase in mobility or a loss of stability. This can frequently be observed clinically because miniscrew threads and marginal bone are mechanically interlocked; this consequently could bring bone along during the displacement.

A limitation of our methodology may be that we did not measure closer to the miniscrew than 0.5 mm. A recent FEM study demonstrated that maximum principal strain had a stronger correlation with failure risk at distances of 0.5 to 1 mm than at 0.5 mm or less from the miniscrew; this may be attributed to the diversity of

maximum principal strains caused by helical fissures of the miniscrew threads.<sup>6</sup> Consistent with this study and the limitation of DIC systems that cannot measure in the areas that are immediately adjacent to the miniscrew, we excluded the bone surface sites that were in contact with miniscrews to prevent errors in strain values.

Digital image correlation evaluates strains at the bone surface and cannot make statements about strains surrounding the miniscrew at deeper levels. However, because the majority of the screw retention comes from the most superficial cortical layer, it can be assumed to be a close proxy measure of strains immediately below the bone surface. Additionally, we did not model soft tissues in this study, and also the viscoelastic property of the mucosal layer was not included. It may be that their biomechanical behavior can not only influence the intensity of the strain but also change the direction of the strain distribution.<sup>29</sup>

In our study, composite analog bone models were selected to match the mandibular posterior region in cortical plate thickness<sup>30</sup> and other important properties such as Young’s modulus value of cortical plate<sup>31</sup> and cancellous bone.<sup>32</sup> These replicated bone models provided less variability and more consistent geometric and structural properties that allowed for biomechanical analyses that otherwise would have been difficult with a human cadaver, formalin fixed bones, or animal models.<sup>33</sup> Composite analog bone blocks also offer the advantages of easy availability, simple and safe handling, nondegradable properties, and consistency for standardization in biomechanical analyses.<sup>34</sup> The strain values reported here were lower than those in previous studies.<sup>6,20,21</sup> This may be in part due to the stiffness of our analog bone models, which were matched with a frozen fresh human jawbone. The fact that most fresh jawbones in the studies came from subjects between the ages of 59 and 90 years may explain in part the increase in stiffness and the

decrease in viscoelastic energy dissipation that can be expected. Because we used an artificial analog bone model, future studies with animal or human jawbones may be able to more precisely measure the actual strain values at which greater miniscrew failures can be expected.

The clinical ramifications of this study should be clear at this point. It is favorable to load miniscrews as close to the bone surface as possible. Hence, preference should be given to implant designs with reasonably short collar heights and to insertion sites with thin to only moderately thick gingival tissue. Sites with excessively thick or highly mobile soft tissues should be avoided because they preclude an insertion resulting in a favorable loading scenario. If, because of clinical circumstances, a miniscrew does protrude excessively, care should be taken to apply a reduced load, which will create a tipping moment ideally not to exceed the 900 cN·mm level.

## CONCLUSIONS

Strains generated at the bone surface close to a miniscrew are directly related to the moment of the force applied to the miniscrew head. Therefore, both the loading force and the distance at which this force is applied will play roles in the stability of the miniscrew. Among other reasons, the palate appears to be an ideal site for miniscrew insertion because it allows strain distribution over a larger area without interfering with other anatomic structures. Future studies are needed to determine the exact relationship between the human jawbone, bone surface strain generated, tipping forces, and success rates.

## ACKNOWLEDGMENTS

We thank Dentaureum for supplying the miniscrews used in this study.

## REFERENCES

- Büchter A, Wiechmann D, Gaertner C, Hendrik M, Vogeler M, Wiesmann HP, et al. Load-related bone remodeling at the interface of orthodontic micro-implants. *Clin Oral Implants Res* 2006;17:714-22.
- Büchter A, Wiechmann D, Koerdt S, Wiesmann HP, Piffko J, Meyer U. Load-related implant reaction of mini-implants used for orthodontic anchorage. *Clin Oral Implants Res* 2005;16:473-9.
- Nalla RK, Stolken JS, Kinney JH, Ritchie RO. Fracture in human cortical bone: local fracture criteria and toughening mechanisms. *J Biomech* 2005;38:1517-25.
- Schileo E, Taddei F, Cristofolini L, Viceconti M. Subject-specific finite element models implementing a maximum principal strain criterion are able to estimate failure risk and fracture location on human femurs tested in vitro. *J Biomech* 2008;41:356-67.
- Torcasio A, Zhang X, Van Oosterwyck H, Duyck J, van Lenthe GH. Use of micro-CT-based finite element analysis to accurately quantify peri-implant bone strains: a validation in rat tibiae. *Bio-mech Model Mechanobiol* 2012;11:743-50.
- Albogha AH, Kitahara T, Todo M, Hyakutake H, Takahashi I. Maximum principal strain as a criterion for prediction of orthodontic mini-implants failure in subject-specific finite element models. *Angle Orthod* 2016;86:24-31.
- Hung PC, Voloshin AS. In-plane strain measurement by digital image correlation. *J Braz Soc Mech Sci Eng* 2003;25:215-21.
- Tiozzi R, de Torres EM, Rodrigues RC, Conrad HJ, de Mattos Mda G, Fok AS, et al. Comparison of the correlation of photoelasticity and digital imaging to characterize the load transfer of implant-supported restorations. *J Prosthet Dent* 2014;112:276-84.
- Tiozzi R, Lin L, Rodrigues RC, Heo YC, Conrad HJ, de Mattos Mda G, et al. Digital image correlation analysis of the load transfer by implant-supported restorations. *J Biomech* 2011;44:1008-13.
- Vaananen SP, Amin Yavari S, Weinans H, Zadpoor AA, Jurvelin JS, Isaksson H. Repeatability of digital image correlation for measurement of surface strains in composite long bones. *J Biomech* 2013;46:1928-32.
- Pan B, Xie H, Yang L, Wang Z. Accurate measurement of satellite antenna surface using 3D digital image correlation technique. *Strain* 2009;45:194-200.
- Berfield TA, Patel JK, Shimmin RG, Braun PV, Lambros J, Sottos NR. Micro- and nanoscale deformation measurement of surface and internal planes via digital image correlation. *Exp Mech* 2007;47:51-62.
- Melenka GW, Nobes DS, Major PW, Carey JP. Three-dimensional deformation of orthodontic brackets. *J Dent Biomech* 2013;4:1758736013492529.
- Windisch SI, Jung RE, Sailer I, Studer SP, Ender S, Hammerle CH. A new optical method to evaluate three-dimensional volume changes of alveolar contours: a methodological in vitro study. *Clin Oral Implants Res* 2007;18:545-51.
- Roberts WE, Vicilli RF, Chang C, Katona TR, Paydar NH. Biology of biomechanics: finite element analysis of a statically determinate system to rotate the occlusal plane for correction of a skeletal Class III open-bite malocclusion. *Am J Orthod Dentofacial Orthop* 2015;148:943-55.
- Mihalko WM, May TC, Kay JF, Krause WR. Finite element analysis of interface geometry effects on the crestal bone surrounding a dental implant. *Implant Dent* 1992;1:212-7.
- Roberts WE, Helm FR, Marshall KJ, Gongloff RK. Rigid endosseous implants for orthodontic and orthopedic anchorage. *Angle Orthod* 1989;59:247-56.
- Roberts WE, Nelson CL, Goodacre CJ. Rigid implant anchorage to close a mandibular first molar extraction site. *J Clin Orthod* 1994;28:693-704.
- Roberts WE, Smith RK, Zilberman Y, Mozsary PG, Smith RS. Osseous adaptation to continuous loading of rigid endosseous implants. *Am J Orthod* 1984;86:95-111.
- Isidor F. Histological evaluation of peri-implant bone at implants subjected to occlusal overload or plaque accumulation. *Clin Oral Implants Res* 1997;8:1-9.
- Melsen B, Lang NP. Biological reactions of alveolar bone to orthodontic loading of oral implants. *Clin Oral Implants Res* 2001;12:144-52.
- Meyer U, Joos U, Myhilli J, Stamm T, Hohoff A, Stratmann U, et al. Ultrastructural characterization of the implant/bone interface of immediately loaded dental implants. *Biomaterials* 2004;25:1959-67.
- Meyer U, Wiesmann HP, Meyer T, Schulze-Osthoff D, Jasche J, Kruse-Losler B, et al. Microstructural investigations of

- strain-related collagen mineralization. *Br J Oral Maxillofac Surg* 2001;39:381-9.
24. Karagiolidou A, Ludwig B, Pazera P, Gkantidis N, Pandis N, Katsaros C. Survival of palatal miniscrews used for orthodontic appliance anchorage: a retrospective cohort study. *Am J Orthod Dentofacial Orthop* 2013;143:767-72.
  25. Nordin M, Frankel VH. *Basic biomechanics of the musculoskeletal system*. 4th ed. Philadelphia: Lippincott Williams & Wilkins; 2012.
  26. Lin TS, Tsai FD, Chen CY, Lin LW. Factorial analysis of variables affecting bone stress adjacent to the orthodontic anchorage mini-implant with finite element analysis. *Am J Orthod Dentofacial Orthop* 2013;143:182-9.
  27. Suzuki A, Masuda T, Takahashi I, Deguchi T, Suzuki O, Takano-Yamamoto T. Changes in stress distribution of orthodontic mini-screws and surrounding bone evaluated by 3-dimensional finite element analysis. *Am J Orthod Dentofacial Orthop* 2011;140:273-80.
  28. Kelly N, Harrison NM, McDonnell P, McGarry JP. An experimental and computational investigation of the post-yield behavior of trabecular bone during vertebral device subsidence. *Biomech Model Mechanobiol* 2013;12:685-703.
  29. Stokes I, Greenapple DM. Measurement of surface deformation of soft tissue. *J Biomech* 1985;18:1-7.
  30. Baumgaertel S, Hans MG. Buccal cortical bone thickness for mini-implant placement. *Am J Orthod Dentofacial Orthop* 2009;136:230-5.
  31. Van Staden RC, Guan H, Loo YC. Application of the finite element method in dental implant research. *Comput Methods Biomech Biomed Engin* 2006;9:257-70.
  32. Misch CE, Qu Z, Bidez MW. Mechanical properties of trabeculae bone in the human mandible: implications for dental implant treatment planning and surgical placement. *J Oral Maxillofac Surg* 1999;57:700-6.
  33. Dunlap JT, Chong AC, Lucas GL, Cooke FW. Structural properties of a novel design of composite analogue humeri models. *Ann Biomed Eng* 2008;36:1922-6.
  34. Christofolini L, Viceconti M. Mechanical validation of whole bone composite tibia models. *J Biomech* 2000;33:279-88.